Towards High-resolution Inertial Sensors Employing Parametric Modulation in Coupled Micro-mechanical Resonators

Chun Zhao,[1,2,*] Xin Zhou,[1,3] Milind Pandit,[1] Guillermo Sobreviela,[1] Sijun Du,[1,4] Xudong Zou,[5,6] and Ashwin Seshia[1,†]

[1] *The Nanoscience Centre, Department of Engineering, University of Cambridge, Cambridge, UK, CB3 0FF*
[2] *MOE Key Laboratory of Fundamental Physical Quantities Measurement & Hubei Key Laboratory of Gravitation and Quantum Physics, PGMF and School of Physics, Huazhong University of Science and Technology, Wuhan, China, 430074.*
[3] *National University of Defense Technology, Changsha, China, 410073*
[4] *Department of Electrical Engineering and Computer Sciences, University of California, Berkeley, CA, USA 94720*
[5] *State Key Laboratory of Transducer Technology, Institute of Electronics, Chinese Academy of Sciences, Beijing, China, 100190*
[6] *School of Electronics, Electrical, and Communication Engineering, University of Chinese Academy of Sciences, Beijing, China, 10090*

(Dated: August 15, 2019)

Highly accurate MEMS inertial sensors have a wide range of potential applications, including inertial navigation and seismometry. Conventional approaches to the implementation of inertial sensors reply on transducers that convert the external acceleration into changes in displacement of a proof mass or shifts in resonant frequencies. Recently, it has been demonstrated that inertial forces can also be measured through monitoring spatial energy distribution between two coupled micro-resonators. To extend this approach, we show that a weak dynamic coupling can be established through periodic modulation of the stiffness for a mechanically coupled microresonator system integrated as part of an accelerometer, enhancing the scale factor and resolution of the accelerometer. The resulting capability of parametric modulation also enabled the tuning of the operating point of the accelerometer through the modulation frequency. Utilizing this technique, we show that the scale factor of the accelerometer can be enhanced by a factor of 188, and a factor of 25 improvement in sensor resolution is demonstrated. Dynamic tuning of the sensor scale factor and inherent noise filtering is also demonstrated.

INTRODUCTION

Rapid advances in micro/nanoelectromechanical systems have enabled a plethora of low-cost miniaturized sensors [1–3], enabling a wide variety of automotive, consumer and healthcare applications. There is increasing interest in applications that demand higher accuracy measurements. In this context, the paradigm of mode-localized sensing [4] was recently proposed. Mode-localized sensing employs the principle of vibration mode-localization in coupled resonators in a sensing context with consequent advantages of passive common-mode rejection [5] and high parametric sensitivity [6, 7]. The underlying principles of vibration mode-localization [8] are essentially similar to Anderson localization observed in the context of electron wave localization in a semiconductor lattice [9].

In a typical mode-localized sensor (see Fig. 1), the measurand is transduced by measuring the effects of induced asymmetry in a system of nearly identical coupled resonators. In practice, one of the system parameters (i.e. in the form of stiffness or mass) on one of the resonators; this resonator is part of a system of weakly coupled nearly identical resonators. This disruption in symmetry (most simply reproduced in a two-degree-of-freedom system [6], modeled as in Fig. 1b) leads to spatial vibration energy confinement in the coupled system. An intuitive manifestation of the spatial energy redistribution is the perturbed extended mode shape, and this can be practically recorded by measuring the relative amplitude of vibration (or amplitude quotient [10]) of the two resonators in a specified mode (see Fig. 1d).

The coupling element is crucial to the scale factor (and resolution) of the sensor, as minimizing the coupling strength optimizes the sensor performance. However, in practice, it is difficult to control the coupling between the resonators. Electrostatic coupling elements [6] offer the advantage of voltage tunability, but it is subject to the risk of dynamic pull-in, especially when the resonators undergo mechanical loading in the context of inertial sensor applications. Mechanical coupling [4], on the other hand, mitigates this risk, but suffers from its low tunability.

Recently, there is much interest in parametric modulation techniques to manipulate the coupling element in coupled micro- and nanoscale resonators [11–14]. In this paper, for the first time, we propose a new sensing paradigm, utilizing the parametric modulation approach to minimize the coupling within a coupled resonant sensing element, in the context of acclerometer. This new ap-

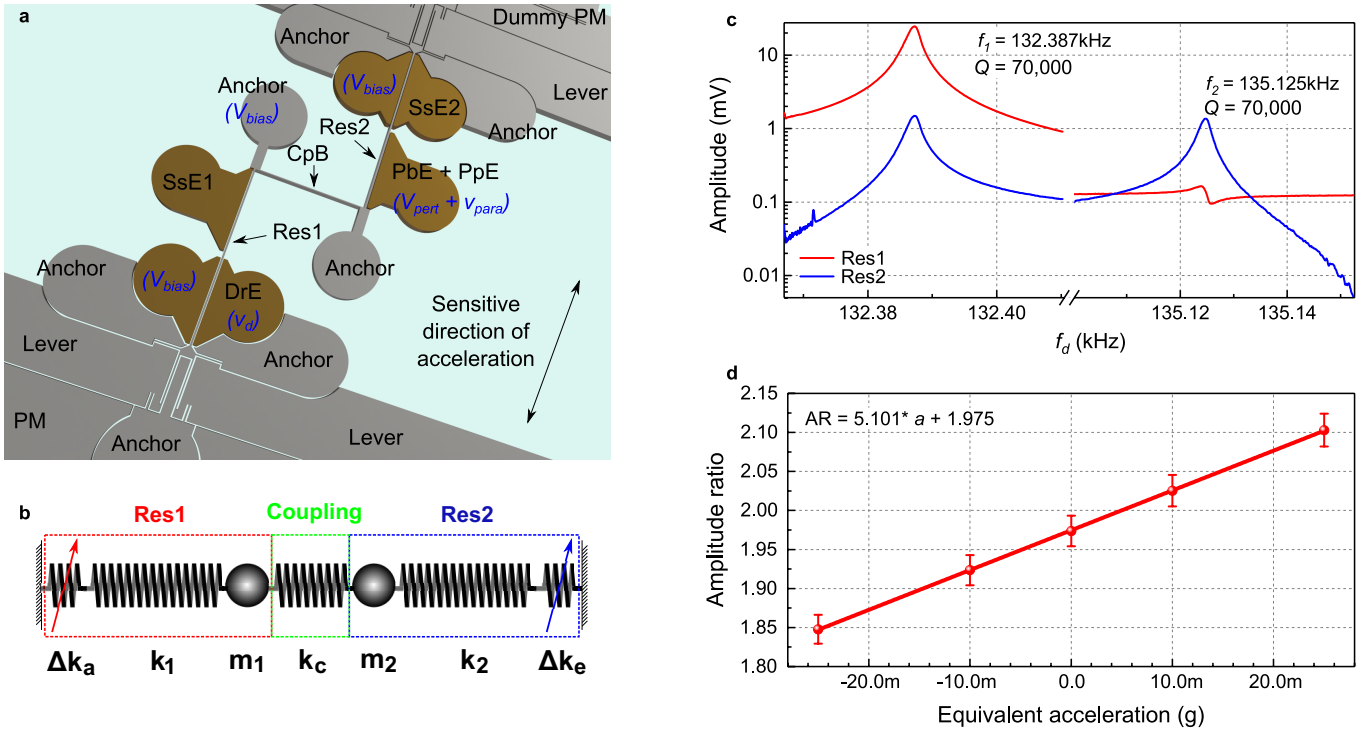

FIG. 1. **2DoF mode-localized resonant accelerometer, detailed device information can be found in Supplementary information.** (a) Illustration of the device layer structures of the vacuum packaged sensor. (b) The spring-mass model of the two resonator system. (c) Measured initial open-loop responses ($v_{para} = 0, V_{pert} = 0$), with respect to drive signal frequency f_d; (d) Measured amplitude ratio x_1/x_2 with respect to a change in equivalent acceleration with $V_{pert} = -20$V.

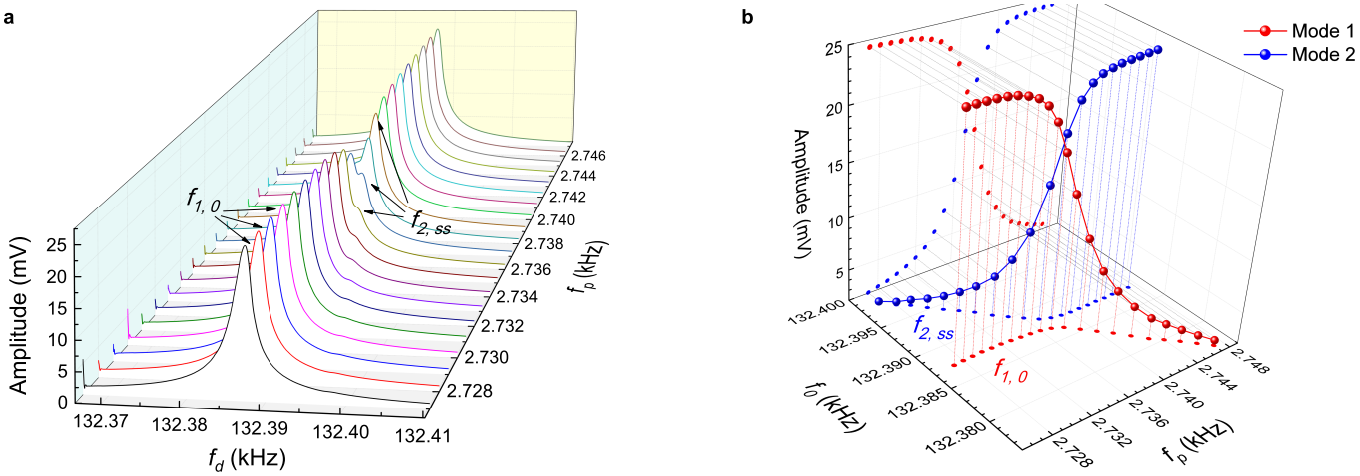

FIG. 2. **Open-loop characterizations of the 2DoF mechanically coupled resonator system, with parametric pump on.** (a) Measured open loop frequency response of resonator 1 in close vicinity of the first mode (f_1) by sweeping drive frequency f_d. The drive voltage has an amplitude of 500μV, and the amplitude of the parametric pump signal is maintained at 400mV; (b) The extracted peak amplitude and mode frequency of the two coupling modes of resonator 1, with respect to a varying f_p. From the projections of the curves on the (f_p, amplitude) plane.

proach allows for a tunable scale factor, significant gains in resolution, inherent noise filtering, and paves the way for several new features to be added to sensors based on coupled resonator architectures..

PARAMETRIC MODULATION IN COUPLED RESONATORS

Similar to the approach described in [12], the displacement of each resonator can be transformed into the dis-

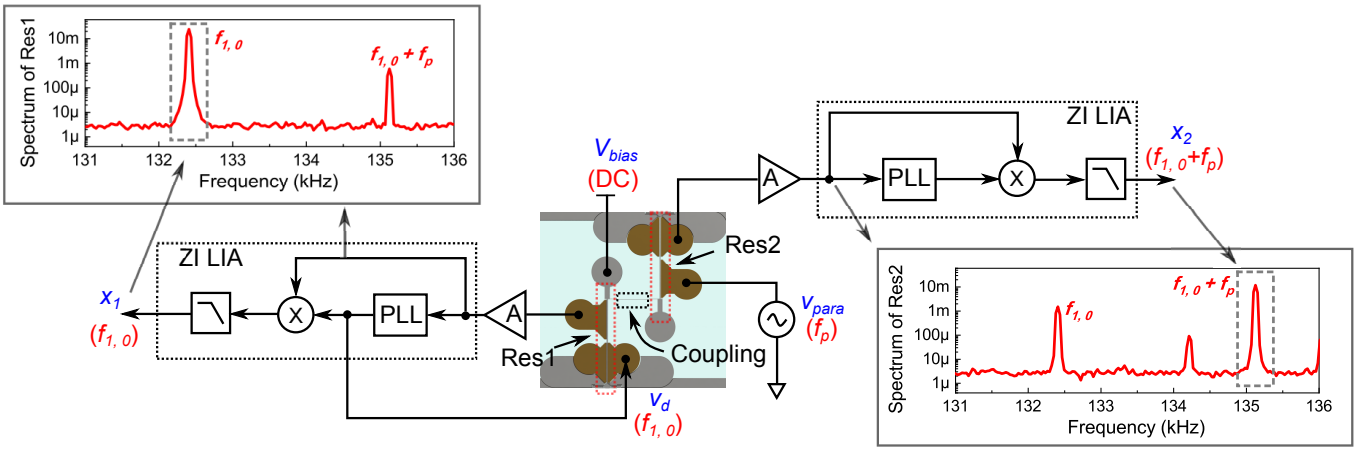

FIG. 3. **Closed-loop experimental setup.** The drive signal v_d is generated using the PLL from Res1 at the frequency of $f_{1,0}$; the Res1 amplitude is measured at the frequency of $f_{1,0}$; and the Res2 amplitude is measured at the frequency of $f_{1,0}+f_p$.

placement of the system of each mode, X_i ($i = 1, 2$, ith mode). Upon introducing the parametric pump at the frequency of f_p, the dynamics of a two-degree-of-freedom (2DoF) weakly coupled resonator system can be written in terms of the displacement of two vibrational modes, X_i:

$$M\ddot{X}_1 + c\dot{X}_1 + [k_{\text{eff},1} + \Gamma_1 \cos(2\pi f_p t)]\, X_1 + \Lambda \cos(2\pi f_p t) X_2 = F_1 \cos(2\pi f_d t + \phi) \tag{1a}$$

$$M\ddot{X}_2 + c\dot{X}_2 + [k_{\text{eff},2} + \Gamma_2 \cos(2\pi f_p t)]\, X_2 + \Lambda \cos(2\pi f_p t) X_1 = F_2 \cos(2\pi f_d t + \phi) \tag{1b}$$

where M is the effective mass of the resonators, c is the damping coefficient of the resonators (both are assumed identical), $k_{\text{eff},i}$ is the effective stiffness of the ith mode, F_i is the drive force of the ith mode, f_d is the drive signal frequency, Γ_i and Λ are the intra- and inter-modal coupling terms, respectively, arising from the mechanical coupling and parametric excitation. The coupling terms can be derived using the theory presented in [12]:

$$\Gamma_1 = \frac{k_p}{2} \frac{\sqrt{(\Delta k)^2 + 4k_c^2} + (\Delta k)^2}{\sqrt{(\Delta k)^2 + 4k_c^2}} \tag{2a}$$

$$\Gamma_2 = \frac{k_p}{2} \frac{\sqrt{(\Delta k)^2 + 4k_c^2} - (\Delta k)^2}{\sqrt{(\Delta k)^2 + 4k_c^2}} \tag{2b}$$

$$\Lambda = \frac{k_p}{2} \frac{k_c}{\sqrt{(\Delta k)^2 + 4k_c^2}} \tag{2c}$$

where k_p is the effective stiffness magnitude of the stiffness modulation applied on the resonator. These terms can be directly related to the absolute magnitude of the resonator amplitude at the two fundamental modes of resonance. In particular, the inter-modal coupling term, Λ, is the main path of energy transfer between the two modes.

Once a parametric voltage is turned on, normal mode splitting can be observed (see Fig. 2a), with two modes at frequencies of $f_{1,0}$ and $f_{2,ss}$. It can be explained by the coupling between the first fundamental mode and the Stokes-sideband of the second mode. Coupling is evident in by noting that avoided crossing (or frequency veering) occurs (see Fig. 2b, (f_p, f_0) plane). In addition to the frequency tuning, by varying the parametric frequency f_p, energy redistribution between the two coupling modes can be well controlled (see Fig. 2b, (f_p, amplitude) plane).

By fixing a parametric pump voltage with an amplitude of v_{para}, at the frequency of f_p, a specific coupling stiffness is achieved allowing for the fine modulation of energy transfer between the two resonators. This new

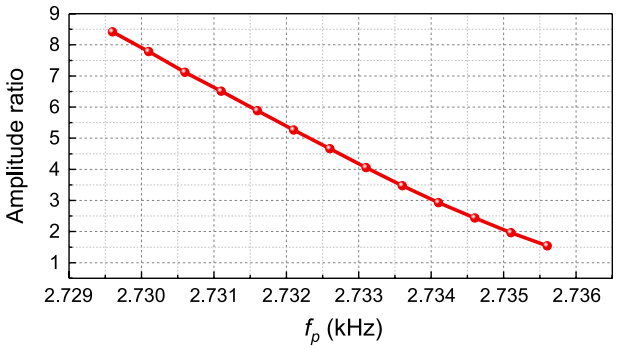

FIG. 4. **Tunability of the operating point.** The operating point can be tuned by adjusting the parametric pump frequency, f_p, while the accelerometer is placed in a horizontal position.

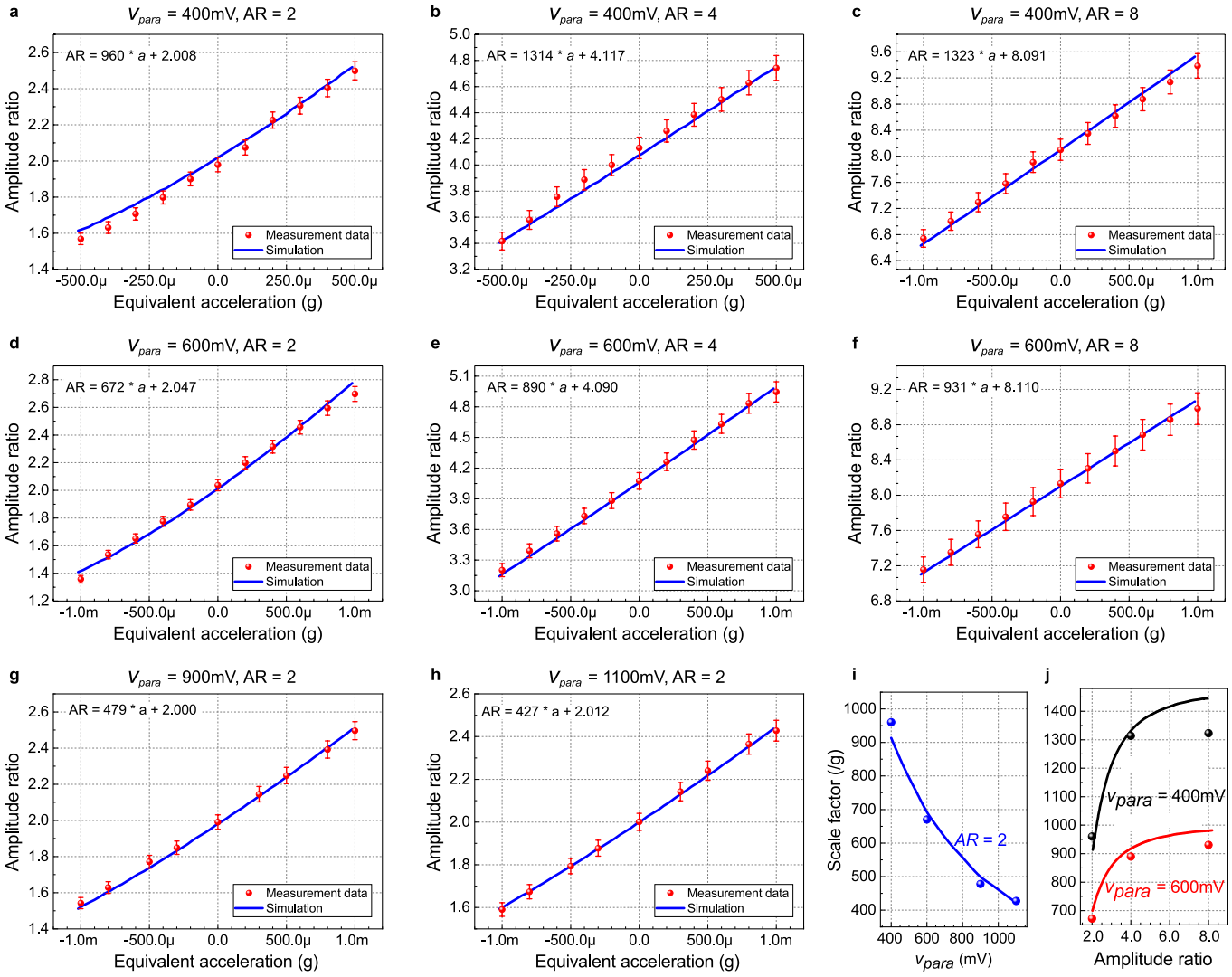

FIG. 5. **Amplitude ratios as a function of an equivalent acceleration in a closed-loop configuration.** (a) - (c) Measured (red) and theoretically calculated (blue) amplitude ratios with v_{para} = 400mV, at different operating points (i.e. amplitude ratios, or AR = 2, 4 or 8). (d) - (f) Measured (red) and theoretically calculated (blue) amplitude ratios with v_{para} = 600mV, at different operating points. (g) - (h) Measured (red) and theoretically calculated (blue) amplitude ratios at the same operating point (i.e. AR = 2) with varying v_{para}. (i) Extracted (dots) and simulated (solid line) scale factors at the same operating point (i.e. AR = 2), as a function of v_{para}. (j) Extracted (dots) and simulated (solid line) scale factors at different operating points.

energy transfer link is much weaker than pure mechanical coupling. This is evident in the extremely small frequency difference seen between the two modes (see Fig. 2). Hence, compared to pure mechanical coupling, the energy redistribution between the resonators is more prominent through this new approach.

PARAMETRIC MODULATION APPROACH UTILIZED FOR ACCELERATION SENSING

Scale factor. With weak energy coupling established through the parametric modulation approach, the energy distribution within the coupled resonator is sensitive to external perturbations, i.e. acceleration in this case. For practical applications, it is necessary to implement a closed-loop measurement configuration (see Supplementary information), and measure the spatial and modal energy redistribution [12]. The measurement metric for closed-loop sensing in this study is therefore the ratio of the amplitude of resonator 1 at $f_{1,0}$ to the amplitude of resonator 2 at $f_{1,0} + f_p$.

The operating point of the sensor can be tuned by adjusting the parametric pump frequency, f_p, as can be seen in Fig. 4. After fixing f_p, the accelerometer can be used for sensing around a desired operating

point. Acceleration change is introduced using a standard tilt test. Due to the small changes in acceleration required (< 1mg), a high resolution tilt platform with a resolution of 2" (TGN80, MKS Instruments, Inc.; a 2" change in angle corresponds to approximately 9.7μg) is used. The step of the tilt applied is 20" (equivalent to 97μg) for $v_{\text{para}} = 400$mV, or 40" (equivalent to 194μg) for $v_{\text{para}} = 600$mV. With the change in acceleration, the stiffness of the Res1 is modified, and spatial energy localization results in a change in the measured amplitude ratio. The calculated amplitude ratio, with respect to the constant equivalent acceleration input is also shown in Fig. 5. Several different configurations of v_{para} and f_p are used. v_{para} is varied from 400mV (see Fig. 5a-c) to 600mV (see Fig. 5d-f), to manipulate the coupling strength. f_p is varied to alter the initial zero-input operating point, e.g. the sensor is adjusted to operate in vicinity of $x_1/x_2 = 2$ in Fig. 5a and Fig. 5d. The scale factor of the device for different operating conditions has been extracted and displayed in each individual figure.

With this approach, significant improvement in the scale factor can be observed, through using the parametric modulation approach. Compared to pure mechanical coupling, at a similar operating point of $x_1/x_2 = 2$, the scale factor enhancement using a parametric pump amplitude of 400mV and 600mV is 188 and 132 times, respectively.

In addition to the significant improvement in the scale factor, another major advantage of this approach is the capability of tuning the scale factor, which can be achieved using two methods. The first method is by changing the amplitude of parametric pump, v_{para}, as can be seen in Fig. 5i. By increasing v_{para} from 400mV to 1100mV, the scale factor is reduced by 50%, as predicted by the theory. Further reduction in coupling strength is theoretically possible by reducing v_{para}. However, this is practically undesired, due to fact that the frequency difference becomes less than the line width, which is defined by the damping in the mechanical resonators. Energy dissipation in the resonators is non-negligible and modal overlap limits quantification of the variations in amplitude ratios. For this reason, in other studies, it is also recommended that the frequency split should be larger than the damping rate [15].

Noise floor. The output noise floor of the sensor, utilizing the parametric modulation approach, is measured in a low noise environment (British Geographic Survey observatory in Eskdalemuir, Scotland), hence isolating the ambient vibrations, as well as in the University laboratory environment, where ambient vibrations due to scientific equipment, external traffic and construction, and other sources is inevitable. The processed output noise power spectral density (NPSD) for $v_{para} = 400$mV and AR= 2 is presented in Fig. 6a. The two processed NPSD (processed in the University lab and at the low-noise site) matched well, except for a few peaks, e.g. at approximately 8Hz, which are thought to result from ambient vibrations in the University laboratory environment. Excluding this, the NPSD processed from the data measured in a low noise environment is representative of the intrinsic noise of the existing experimental setup.

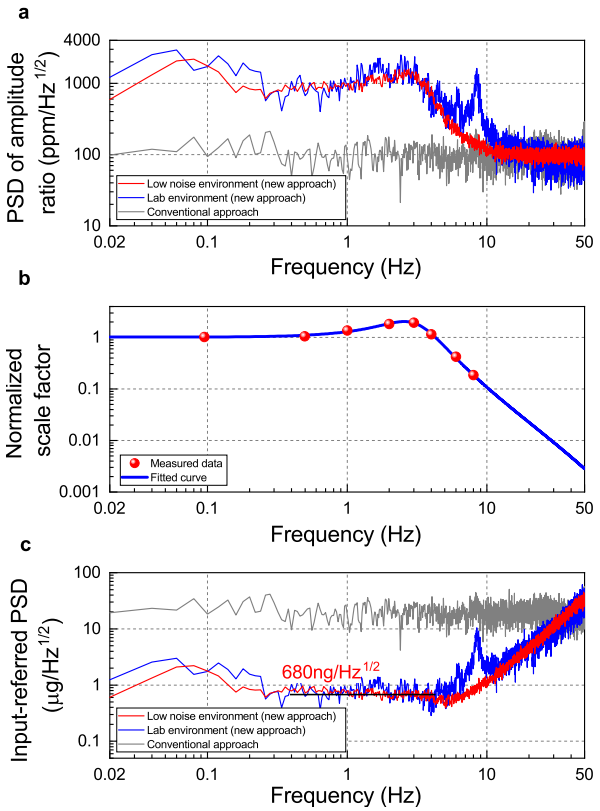

FIG. 6. **Dynamic response of the sensor**, (a) Measured output NPSD of the accelerometer; (b) measured dynamic scale factor using the parametric modulation approach, normalized to the DC scale factor; (c) the input-referred NPSD of the accelerometer calculated using measured output PSD and scale factor.

The dynamic scale factor of the sensor is measured by applying an alternating electrostatic force to the proof mass through an additional set of electrodes, to mimic an equivalent acceleration induced force. A plot of the scale factor versus the frequency of input acceleration is shown in Fig. 6b. The measured scale factor is fitted to a high-order transfer function also shown in Fig. 6b. It can be observed from the figure that the scale factor decreases as the frequency of input acceleration increases. This inherent noise filtering feature is another major benefit of the parametric modulation approach proposed in this paper.

The input-referred NPSD in terms of acceleration is estimated using both the measured output NPSD and estimated scale factor, and is shown in Fig. 6c. The estimated noise floor of the accelerometer using parametric modulation approach is 680ng/Hz$^{1/2}$, over a frequency

span between 0.5Hz to 3Hz.

In comparison, the output NPSD using the conventional mode-localized approach is shown in Fig. 6a. Since the scale factor of the conventional approach is constant at frequencies below the frequency difference [16], which is approximately 2.7kHz in this case, the input-referred PSD of the accelerometer without parametric modulation can be estimated using the DC scale factor of 5.1 (see Fig. 1d), and is shown in Fig. 6c. Using the conventional approach, the input-referred noise floor is approximately 17.5μg/Hz$^{1/2}$ in the same device. Thus, a significant improvement of approximately 25 times in resolution is obtained using the parametric modulation approach, demonstrating the step-change improvement in performance achievable by employing this approach.

Sensor bandwidth. As shown in Fig. 6b, the scale factor depends on the input frequency, revealing another advantage of this proposed sensing scheme, in providing for inherent filtering of high-frequency background noise. Since the dynamic scale factor matched well with the output NPSD measurements in Fig. 6, an NPSD based bandwidth measurement technique is employed here to characterize the signal bandwidth under different test conditions; these results are shown in Fig. 7. The measured NPSD is fitted to the same order transfer function model as in Fig. 6b, and illustrated in the figure as well. Typically, for NPSD curves showing resonant behavior, the resonant peak is a good indicator of the signal bandwidth; therefore, the resonant peaks are also marked in the figure. As demonstrated in Fig. 7a, altering the parametric pump amplitude v_{para} while maintaining the same operating point can result in a shift in the noise peak frequency, thus the noise bandwidth. By varying v_{para} from 400mV to 900mV, the resonant peak frequency is increased by approximately 73%. Alternatively, maintaining the value of v_{para} and changing the operating point is another effective method for tuning the operational bandwidth. By changing the operating point from AR=2 to AR=8 (corresponding to the parametric pump frequency, f_p, changing from 2735Hz to 2730Hz), the resonant peak frequency is increased by over 170%. Both approaches are, thus, effective in allowing for tuning of the operational bandwidth.

This system is the classical analogue of a two-state quantum system describing the Landau-Zener transition [17, 18]. Note that, for the case considered in Fig. 7 above, the device is subject to white noise excitation due to Brownian noise and other external noise sources (e.g. voltage sources) present in the system. The response to low-frequency excitation can be modeled as an adiabatic transition (classical mode-localized sensing context) while higher frequency excitation can be modeled as a diabatic transition where energy exchange between the resonators is inhibited [15]. The peaks occur, likely because of the corresponding stiffness modulation frequency is coincident with the condition for coherent energy transfer between the modes, and the peak response frequency is determined by the frequency split between the two newly established modes, i.e. $f_{1,0}$ and $f_{2,ss}$, due to the application of parametric pump (see supplementary materials).

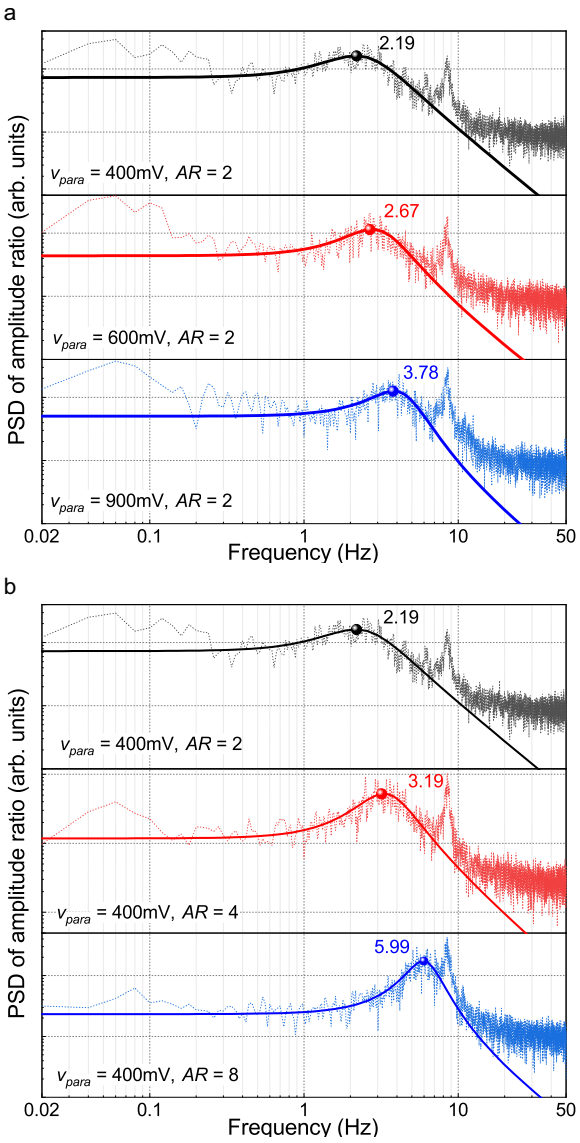

FIG. 7. **Tunable filtering capabilities of the accelerometer**. (a) Measured (dotted lines) and fitted (solid lines) PSD of the sensor near the same operating point of AR= 2, with different parametric pump amplitudes, v_{para}. (b) Measured (dotted lines) and fitted (solid lines) PSD of the sensor near different operating points, i.e. AR= 2, 4 or 8 (thus altering parametric pump frequency, f_p), with identical v_{para}.

As noted above, when the noise force modulation frequency matches the condition for coherent energy transfer between the modes, a scale factor enhancement is seen. For instance, for v_{para} = 400mV and AR = 8, the noise amplification at 5.99Hz is over 7 times higher than near DC frequencies (see Fig. 7b), while the peak

frequency coincides with the frequency split between $f_{1,0}$ and $f_{2,ss}$ (see Supplementary materials). Since the NPSD plot is representative of the dynamic scale factor (as shown in Fig. 6a and b), this phenomenon indicates that the scale factor can be enhanced at the coherent energy transfer frequency, which can be tuned by changing v_{para} and f_p. Further detailed theoretical studies will be required to fully investigate this effect, as well as the practicalities of operating precisely at this peak response point.

DISCUSSIONS

From Fig. 7, it can be seen that the fundamental resolution limit to the existing sensor is the noise intrinsic to the experimental setup. With the parametric modulation approach, the scale factor is over two orders of magnitude higher than the conventional mode-localized case. Factors limiting measurements could include the noise inherent to the polarization voltage and parametric pump signal, as well as fluctuations in the ambient temperature. However, it is believed that these factors can be much better isolated through further optimization of the test configurations, including specifically designing a low noise polarization voltage source based on low-dropout voltage regulators, and suitable temperature control/compensation. If these factors are isolated from the test configuration, the sensor will then be limited by the front-end electronics.

Thus, with further optimization of the test configuration, the output PSD of the conventional mode-localized approach is likely to be limited only by the front-end electronics. Therefore, the noise floor of the front-end electronics can be estimated from Fig. 7a (depicted in gray), which is approximately 89ppm/$\text{Hz}^{1/2}$ between 1 to 50Hz. Additionally, through further optimization of the MEMS device design, the thermo-mechanical noise floor could be reduced [2], and under the assumption that the front-end electronics noise dominates, the projected input-referred noise floor of this particular sensor can be estimated using the measured scale factor in Fig. 7b. Using the measurements of amplitude ratio noise (as limited by the front-end electronics), a low noise floor of 50ng/$\text{Hz}^{1/2}$ between 2-3Hz can potentially be achieved. Therefore, it is necessary to further isolate the aforementioned noise sources, in order to achieve this low noise floor. Furthermore, it should be pointed out that the device design (e.g. resonator design, proof mass and suspension design), as well as the front-end electronics can be optimized, potentially achieving even better performance in future iterations of these devices.

CONCLUSIONS

We report a practical application of the parametric modulation technique, towards enhancing the scale factor and resolution of mode-localized MEMS accelerometers, as well as high tunability in scale factor and operational bandwidth. Utilizing this approach, key challenges with existing mode-localized MEMS sensor technology can be elegantly solved. Most important of all, we have shown that the inter-modal coupling can be manipulated, and reduced specifically, with this approach, by orders of magnitude to achieve an improved scale factor, and thus an enhanced resolution. In particular, we show that 188 times improvement in scale factor can be achieved in this particular device, enabling a noise floor of 680ng/$\text{Hz}^{1/2}$, which is over one order of magnitude lower relative to the conventional mode-localized approach. Assuming that the front-end interface electronics noise dominates, this noise floor could potentially reach 50ng/$\text{Hz}^{1/2}$. Further improvements of the resolution can be enabled by improving the Q-factor of the resonators to allow for even weaker coupling strength. Also, the continuing optimization of the device design and electronics can further improve the electronics noise limited resolution.

Additionally, this approach allows for tuning of the operating point by varying the parametric pump frequency, while also enabling the control of scale factor. Frequency tuning can potentially provide more robust and precise tuning, compared to conventional electrostatic tuning approach using a voltage. Furthermore, the operating point is predominantly determined by the parametric pump frequency, which can be generated with a much higher long-term stability compared to DC voltages. Low noise, high stability and compact MEMS frequency references can be easily integrated without changing much of the form factor of the sensor system. In conjunction with scale factor tuning through parametric pump amplitude, this proposed sensing scheme can find its potential application in sensing systems where accurate matching of scale factor is necessary [19].

One more feature of this new approach is the signal filtering, or frequency dependent scale factor, with potentially significant improvements in terms of scale factor obtainable by operating at a specific frequency. One potential advantage of this is the possibility of rejecting undesired wide band ambient vibrations or other external systematic noise, while amplifying signals at a desired frequency. It should be pointed out that the operational bandwidth can also be tuned by altering both the parametric pump voltage amplitude or frequency. The results reported here should be followed up in further depth to fully explore the theoretical framework, as well as potential benefits achievable by enabling the filtering of external noise.

However, for a fixed f_p, a drift in $f_1 - f_2$, which is

predominantly affected by the drift in the coupling element (i.e. mechanical coupling in this case), results in a drift in the operating point. Therefore, low ambient dependence coupling beam is necessary to further improve the accelerometer's long-term stability. Additionally, the drift in the pump frequency, f_p could also have a similar effect; thus, a stable frequency reference to generate f_p is desired for long-term stability considerations.

Nevertheless, for the first time, this study shows a potential sensing application for the parametric modulation technique. It should be pointed out that this approach can be extended to other physical systems, e.g. NEMS resonators or optical resonators, in addition to where the coupling between the systems can be similarly tuned for sensing applications, including micromechanical gyroscopes.

ACKNOWLEDGEMENT

Funding from Innovate UK and the Natural Environment Research Council is gratefully acknowledged.

* chun_zhao@hust.edu.cn
† aas41@cam.ac.uk

[1] R. Middlemiss, A. Samarelli, D. Paul, J. Hough, S. Rowan, and G. Hammond, Nature **531**, 614 (2016).
[2] W. Pike, A. Delahunty, A. Mukherjee, G. Dou, H. Liu, S. Calcutt, and I. Standley, in *SENSORS, 2014 IEEE* (IEEE, 2014) pp. 1599–1602.
[3] X. Zou, P. Thiruvenkatanathan, and A. A. Seshia, Journal of Microelectromechanical Systems **23**, 768 (2014).
[4] M. Spletzer, A. Raman, A. Q. Wu, X. Xu, and R. Reifenberger, Applied Physics Letters **88**, 254102 (2006), doi: 10.1063/1.2216889.
[5] P. Thiruvenkatanathan, J. Yan, and A. A. Seshia, IEEE transactions on ultrasonics, ferroelectrics, and frequency control **57**, 690 (2010), doi: 10.1109/TUFFC.2010.1466.
[6] P. Thiruvenkatanathan, J. Yan, J. Woodhouse, and A. A. Seshia, Journal of Microelectromechanical Systems **18**, 1077 (2009), doi: 10.1109/JMEMS.2009.2025999.
[7] P. Thiruvenkatanathan, J. Yan, J. Woodhouse, A. Aziz, and A. Seshia, Applied Physics Letters **96**, 081913 (2010).
[8] C. Pierre, Journal of Sound and Vibration **126**, 485 (1988).
[9] P. W. Anderson, Physical review **109**, 1492 (1958).
[10] C. Zhao, G. S. Wood, J. Xie, H. Chang, S. H. Pu, and M. Kraft, Journal of Microelectromechanical Systems **25**, 626 (2016).
[11] T. Faust, J. Rieger, M. J. Seitner, J. P. Kotthaus, and E. M. Weig, Nature Physics **9**, 485 (2013).
[12] H. Okamoto, A. Gourgout, C.-Y. Chang, K. Onomitsu, I. Mahboob, E. Y. Chang, and H. Yamaguchi, Nature Physics **9**, 480 (2013).
[13] G. Luo, Z.-Z. Zhang, G.-W. Deng, H.-O. Li, G. Cao, M. Xiao, G.-C. Guo, L. Tian, and G.-P. Guo, Nature communications **9**, 383 (2018).
[14] S. Cho, S. U. Cho, M. Jo, J. Suh, H. C. Park, S. G. Kim, S.-B. Shim, and Y. D. Park, Phys. Rev. Applied **9**, 064023 (2018).
[15] L. Novotny, American Journal of Physics **78**, 1199 (2010).
[16] M. Pandit, C. Zhao, G. Sobreviela, X. Zou, and A. Seshia, "A high resolution differential mode-localized mems accelerometer (submitted)," (2019).
[17] T. Faust, J. Rieger, M. J. Seitner, P. Krenn, J. P. Kotthaus, and E. M. Weig, Physical review letters **109**, 037205 (2012).
[18] M. Frimmer and L. Novotny, American Journal of Physics **82**, 947 (2014).
[19] X. Huang, Z. Deng, Y. Xie, Z. Li, J. Fan, and L. Tu, Sensors **17**, 2471 (2017).